

High resolution Fowler-Nordheim field emission maps of thin silicon oxide layers

Todd G. Ruskell,^{a)} Richard K. Workman, Dong Chen,^{b)} and Dror Sarid
Optical Sciences Center, University of Arizona, Tucson, Arizona 85721

Sarah Dahl and Stephen Gilbert^{c)}
Electrical and Computer Engineering, University of Arizona, Tucson, Arizona 85721

(Received 10 July 1995; accepted for publication 23 October 1995)

An improved method for characterizing thin oxide films using Fowler-Nordheim field emission is reported. The method uses a conducting-tip atomic force microscope with dual feedback systems, one for the topography and a second for the field emission bias voltage. Images of the voltage required to maintain a 10 pA emission current through a 3 nm oxide film thermally grown on *p*-type Si(100) demonstrate a spatial resolution of 8 nm. © 1996 American Institute of Physics. [S0003-6951(96)01801-4]

A key issue of ultra-large-scale integration technology (ULSI) is the quality and reliability of thin silicon oxide layers used in devices. Gate lengths of 180 nm, and oxide thicknesses less than 5 nm will be required as the semiconductor industry pushes toward 1 Gbit memory chips and beyond.¹ High lateral resolution of the local electrical properties of these thin oxides is gaining interest because of some indications that the breakdown fields of gate quality oxides may not be limited by the intrinsic dielectric strength of the oxide, but rather by localized defects in the oxide layer or at the Si-SiO₂ interface.^{2,3} Scanning probe microscopies, derived from the scanning tunneling microscope and atomic force microscope (AFM), are uniquely suited to this type of local interrogation. In particular, conducting probe AFM allows one to perform high resolution scans of insulating surfaces while simultaneously collecting electrical information about the surface. This general technique has been explored for measurements of capacitance,⁴ dopant profiles,⁵ and Fowler-Nordheim (FN) emission currents through oxides.³ This last study demonstrated a novel method of characterizing the pre-breakdown FN emission current of a 12 nm oxide film. For each data point the AFM feedback was turned off, and the voltage across the oxide was increased until a FN emission current threshold of 50 pA was reached. The maximum applied voltage at each point was recorded to produce a 20 nm resolution voltage map, while spending as much as 0.6 s at every data point.

In this letter we report on an improved method that enables us to obtain 8 nm resolution maps of FN emission currents while spending only 40 ms at each data point, which is an order of magnitude faster than previously reported. Figure 1 shows a conventional deflection mode AFM⁶ with a conducting tip measuring the topography of an oxide surface at constant force using a computer-controlled feedback system. A second computer-controlled feedback system⁷ simultaneously monitors the tip-sample FN emission current

through the oxide and adjusts the applied sample bias to maintain a constant 10 pA setpoint current. A 20 GΩ current-limiting resistor was placed in series with the junction, and a pre-amp sensitive to less than 0.5 pA was used to detect the tunneling current. The conducting tip and cantilever, fabricated from 75 μm diameter electrochemically etched tungsten wire, exerted forces of several hundred nN during imaging. A 3 nm thermal oxide was grown on a 5 Ω-cm *p*-type Si(100) substrate to test the system. In this experiment, the sample bias was kept positive to prevent the formation of a depletion region at the Si-SiO₂ interface.

The pre-breakdown FN emission current in a plane parallel metal-oxide-silicon (MOS) capacitor is given by⁸

$$I = A_{\text{eff}} \frac{e^3}{8\pi h \phi} \left(\frac{V}{s} \right)^2 \exp \left(\frac{8\pi \sqrt{2m_{\text{eff}}} \phi^{3/2} s}{3heV} \right). \quad (1)$$

Here A_{eff} is the effective emission area, e the electronic charge, h Planck's constant, s the oxide thickness, ϕ the tip-SiO₂ barrier height, $V(V > \phi)$ the bias across the oxide layer, and m_{eff} the effective electron mass in the oxide.

To calculate the effective emission area appropriate for this geometry, we consider only emission from that part of the tip which is in contact with the oxide. This is reasonable for a first order estimation because the fields radiating from parts of the tip not in contact with the oxide diverge at the oxide surface. The tip-sample contact radius is given by $r_c^3 = (3/4)(k_1 + k_2)FR_{\text{tip}}$, where F is the tip-sample applied force, R_{tip} is the tip radius, and $k_i = (1 - \nu_i^2)/E_i$, where E_i and ν_i are Young's moduli and Poisson's ratio of the tungsten tip and silicon oxide film.⁹ The effective area for tunneling is then given by $A_{\text{eff}} = \pi r_c^2$. A tip radius of 50 nm and forces ranging from 100 to 1000 nN yield contact radii of 3.7 nm to 8 nm, and effective areas of 43 nm² to 201 nm². For smaller contact radii or thicker oxide layers, further modifications to the effective area would be necessary to compensate for the highly nonuniform fields between tip and sample. It is clear from the effective areas calculated above that a meaningful FN map can only be obtained if the effective area remains constant. The AFM feedback loop maintains a constant tip-

^{a)}Electronic mail: todd@bucky.opt-sci.arizona.edu

^{b)}Present address: IBM Manufacturing Technology Center, Boca Raton, FL 33429.

^{c)}Present address: Optical Sciences, University of Arizona.

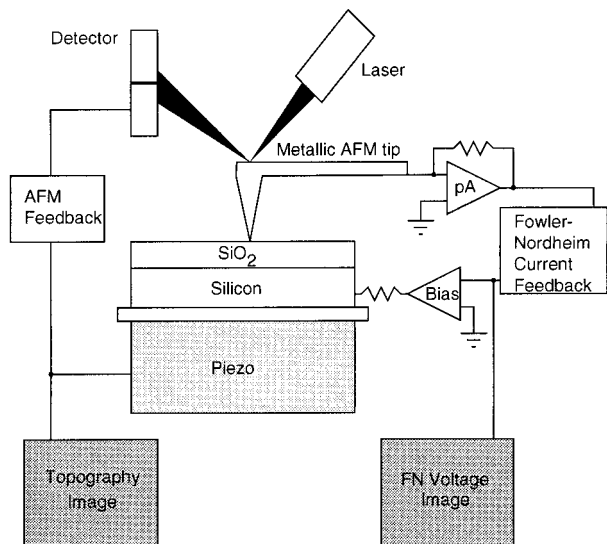


FIG. 1. Schematic diagram of the experimental system. A deflection-mode AFM measures the sample topography while a second feedback system simultaneously records the voltage required to maintain a FN emission current of 10 pA. The tip and sample were electrically isolated from the piezo tube and AFM head.

sample force, and hence effective area, regardless of the bias applied for the FN field emission. This is possible because the AFM feedback loop operates at 62.5 kHz, and the FN feedback loop is operating at only 800 Hz.

Figure 2 shows experimental results of the topography, a voltage map for an FN emission current of 10 pA, and a line scan through the voltage map. This 215 nm \times 215 nm image demonstrates the ability of the system to resolve electrical features as small as 8 nm, in agreement with the effective calculated radius. Although the lateral resolution of this technique is on the order of the thickness of the oxide, in this image a feature 3 nm in size is only one pixel wide, and indistinguishable from noise. The black-to-white contrast on the topographical and voltage images corresponds to 5 nm and 16 V, respectively. The surface, when imaged before applying a bias, displayed a surface roughness of 0.5 nm. The apparent increase in surface roughness after the application of the bias may be due to nonuniform charging of the oxide film. The range of observed voltages demonstrates that the feedback system is capable of preventing a catastrophic breakdown during the scan. Preventing catastrophic breakdowns is critical when probing the electrical properties of oxides in a nondestructive manner. As an additional check of the oxide quality, a representative $I-V$ curve was taken at a single point to ensure that Eq. (1) accurately described the observed tunneling emission both before and after imaging.

The white (dark) areas of the voltage map correspond to high (low) breakdown voltage regions of the oxide. From Eq. (1), the adjustable parameters are A_{eff} , ϕ , m_{eff} and s . The voltage map, then, can be thought of as a measure of the local variation in these four parameters. A_{eff} is kept constant during scanning by the AFM feedback. Local surface charging, which modifies the effective barrier height ϕ , clearly affects the applied bias required to maintain 10 pA of FN tunneling current. Charging of the oxide can also cause

changes in the local effective mass of the electron. Topographical features may or may not correspond with changes in the oxide thickness s or features in the FN image. If the Si-SiO₂ interface is flat, a change in oxide thickness will be seen both in the topography and as a FN image feature. Interface roughness may cause a change in the local oxide thickness that does not appear in the topography, but will appear in the FN image. Local charging can cause apparent topographical features; however, these charge-induced features can be distinguished from real topographical features by comparing topography images taken before and during

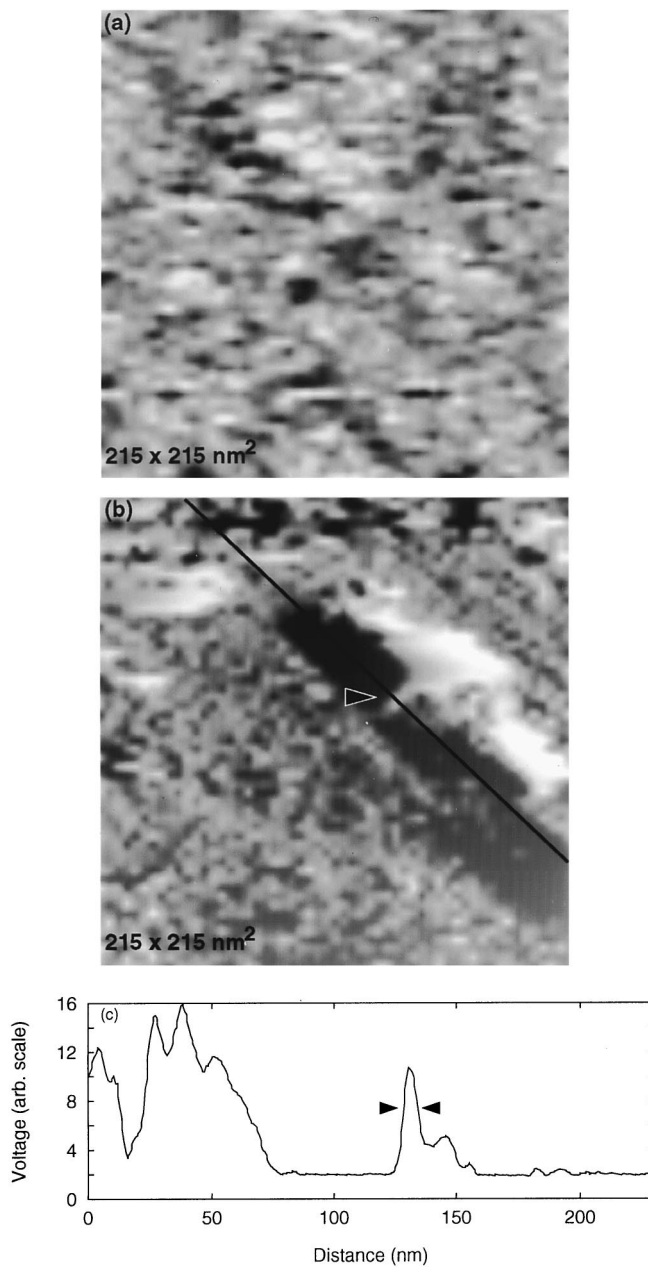


FIG. 2. (a) The surface topography, and (b) map of the voltage required to maintain 10 pA of tunneling current. The contrast in these two images corresponds to 5 nm and 16 V, respectively. No direct correlation is observed between the apparent topography and voltage map. Part (c) shows the profile along the black line drawn on the voltage image. The arrows in (b) and (c) point out an electrical feature 8 nm in size.

the FN imaging. It has been shown that applying a large field between a silicon sample and a conducting tip can lead to additional silicon oxide growth.¹⁰ However, no additional oxide growth was observed during this experiment.

In conclusion, a Fowler-Nordheim emission current feedback system, in conjunction with a conducting tip atomic force microscope, has been developed to probe the lateral pre-breakdown electrical properties of thin oxide films. The system is capable of preventing catastrophic breakdown events, and can produce images with 8 nm resolution. This was made possible by using a feedback system which allows an increase of the scan rate by an order of magnitude over previously reported AFM/FN images of oxide films. The system is currently being used for detailed studies of the breakdown characteristics of contaminated thin oxide films.

We would like to acknowledge helpful discussions with X. Yao and J. Brews. This work is partially supported by the

University of Arizona Center for Microcontamination Control.

¹A. C. Diebold and B. Doris, *Surf. Interface Anal.* **20**, 127 (1993).

²E. Harari, *J. Appl. Phys.* **49**, 2478 (1978).

³M. Murrell, M. Welland, S. O'Shea, T. Wong, J. Barnes, A. McKinnon, M. Heyns, and S. Verhaverbeke, *Appl. Phys. Lett.* **62**, 786 (1993).

⁴C. C. Williams, W. P. Hough, and S. A. Rishton, *Appl. Phys. Lett.* **55**, 203 (1989).

⁵C. Shafai, D. J. Thomson, M. Simard-Normandin, G. Mattiussi, and P. J. Scanlon, *Appl. Phys. Lett.* **64**, 342 (1994).

⁶Digital Instruments, Inc., 520 E. Montecito St., Santa Barbara, CA 93103. Nanoscope III AFM system.

⁷Controlled with software and hardware from Intelligent Instrumentation, 6550 S. Bay Colony Drive, MS130, Tucson, AZ 85706.

⁸R. H. Fowler and L. Nordheim, *Proc. R. Soc. London Ser. A* **119**, 173 (1928).

⁹D. Sarid, *Comp. Mater. Sci.* (in press).

¹⁰E. S. Snow and P. M. Campbell, *Appl. Phys. Lett.* **64**, 1932 (1994).